Molecular basis for the thiol sensitivity of insulin-degrading enzyme

Marie Neant-Fery*, Rubén D. Garcia-Ordoñez*, Todd P. Logan†, Dennis J. Selkoe†, Lilin Li*, Lael Reinstatler‡, and Malcolm A. Leissring*†‡§

*Department of Molecular Therapeutics, The Scripps Research Institute, Scripps Florida, Jupiter, FL 33458; †Center for Neurologic Diseases, Brigham and Women's Hospital, Boston, MA 02115; and ‡Department of Neuroscience, Mayo Clinic College of Medicine, Jacksonville, FL 32224

Edited by Bert L. Vallee, Harvard Medical School, Boston, MA, and approved April 21, 2008 (received for review February 8, 2008)

Insulin-degrading enzyme (IDE) is a ubiquitous zinc-metalloprotease that hydrolyzes several pathophysiologically relevant peptides, including insulin and the amyloid β-protein (Aβ). IDE is inhibited irreversibly by compounds that covalently modify cysteine residues, a mechanism that could be operative in the etiology of type 2 diabetes mellitus (DM2) or Alzheimer's disease (AD). However, despite prior investigation, the molecular basis underlying the sensitivity of IDE to thiol-alkylating agents has not been elucidated. To address this topic, we conducted a comprehensive mutational analysis of the 13 cysteine residues within IDE. Our analysis implicates C178, C812, and C819 as the principal residues conferring thiol sensitivity. The involvement of C812 and C819, residues quite distant from the catalytic zinc atom, provides functional evidence that the active site of IDE comprises two separate domains that are operational only in close apposition. Structural analysis and other evidence predict that alkylation of C812 and C819 disrupts substrate binding, whereas alkylation of C178 interferes with the apposition of active-site domains and subtly repositions zinc-binding residues. Unexpectedly, alkylation of C590 was found to activate hydrolysis of Aβ significantly, while having no effect on insulin, demonstrating that chemical modulation of IDE can be both bidirectional and highly substrate selective. Our findings resolve a long-standing riddle about the basic enzymology of IDE with important implications for the etiology of DM2 and AD. Moreover, this work uncovers key details about the mechanistic basis of the unusual substrate selectivity of IDE that may aid the development of pharmacological agents or IDE mutants with therapeutic value.

Alzheimer's disease | amyloid β-protein | insulin | type 2 diabetes mellitus

Converging lines of evidence strongly implicate insulin-degrading enzyme (IDE) hypofunctionality in the pathogenesis of Alzheimer's disease (AD) and type 2 diabetes mellitus (DM2) (1–3). Multiple, independent genetic studies conducted on populations throughout the world have identified genetic variations in and around the *Ide* gene that are associated with late-onset AD (1, 4–6) and DM2 (7–9). In addition, a rat model of diabetes was found to harbor missense mutations in IDE that decrease its ability to degrade both insulin (10, 11) and amyloid β-protein (Aβ) (10). Likewise, genetic deletion of the *Ide* gene in mice produced elevations in the levels of cerebral Aβ (12, 13) and circulating insulin (12) and, notably, also led to pronounced glucose intolerance (12). Conversely, transgenic overexpression of IDE in neurons potently reduced Aβ levels and prevented amyloid plaque formation and downstream cytopathology in a mouse model of AD (14). Despite these and other compelling findings, functional mutations have not been found in the human *Ide* gene, so it remains to be established how IDE hypofunctionality might arise in the etiology of AD and DM2.

IDE belongs to an evolutionarily distinct superfamily of zinc-metalloproteases with numerous properties that differ from conventional zinc-metalloproteases (15, 16). First, IDE and its homologs feature a zinc-binding motif, HxxEH, that is inverted as compared to the canonical metalloprotease motif, HExxH (17). Second, the subcellular localization of IDE is atypical, being present predominantly in cytosol in addition to peroxisomes and mitochondria (15, 18). There is also abundant evidence that IDE is transported to the extracellular space via a poorly understood, nonclassical secretion pathway (18, 19). Third, the structure of IDE is highly distinctive, consisting of two bowl-shaped halves connected by a flexible linker (20). This structure allows the protease to switch between two conformational states: an "open" state, which allows entry of substrates and exit of products; and a "closed" state, wherein substrates become entrapped within an unusually large internal chamber formed from the N- and C-terminal halves (20).

IDE also differs from conventional zinc-metalloproteases in being sensitive to thiol-modifying agents. The proteolytic activity of IDE is inhibited irreversibly by compounds that covalently modify thiol groups through Michael addition [e.g., *N*-ethylmaleimide (NEM)] or alkylation (e.g., iodoacetamide), while showing a more complex response to thiol-reducing agents such as DTT, being activated by low but inhibited by high concentrations (15). Historically, these properties of IDE, together with conflicting evidence of inhibition by the metal-chelating agent, EDTA (21), substantially delayed its definitive categorization as a metalloprotease. Indeed, IDE was initially officially designated as a cysteine endoproteinase (EC 3.4.22.11) by the Commission on Enzymes of the International Union of Biochemistry (16).

Beyond the purely fundamental significance of this topic, the thiol-sensitive nature of IDE very likely has pathophysiological relevance as well. Several studies have shown that IDE activity is reduced in tissue samples from patients with AD (22, 23) or mild cognitive impairment (23). Importantly, these changes are evident even in the absence of reduced protein levels, suggesting that IDE can be functionally inactivated by disease-relevant posttranslational modifications (22, 23). In this regard, it is highly significant that, in aged mice, IDE has been shown to be alkylated by 4-hydroxynonenal (24), a major lipid peroxidation product that has been shown to inactivate IDE *in vitro* (33). Together, these and other observations suggest that oxidative damage to thiol groups in IDE could play a role in the pathogenesis of age-related diseases such as AD and DM2.

Although the mechanistic basis underlying the thiol sensitivity of IDE is not known, this topic has been investigated. As first noted by Roth and co-workers (25), thiol-sensitive IDE ho-

Author contributions: M.A.L. designed research; M.N.-F., R.D.G.-O., T.P.L., L.L., L.R., and M.A.L. performed research; D.J.S. and M.A.L. contributed new reagents/analytic tools; M.N.-F., T.P.L., L.L., and M.A.L. analyzed data; and D.J.S., L.R., and M.A.L. wrote the paper.

The authors declare no conflict of interest.

This article is a PNAS Direct Submission.

§To whom correspondence should be addressed at: Department of Neuroscience, Mayo Clinic College of Medicine, 4500 San Pablo Road, Birdsall Building, Room 110, Jacksonville, FL 32224. E-mail: leissring@mayo.edu.

This article contains supporting information online at www.pnas.org/cgi/content/full/0801261105/DCSupplemental.

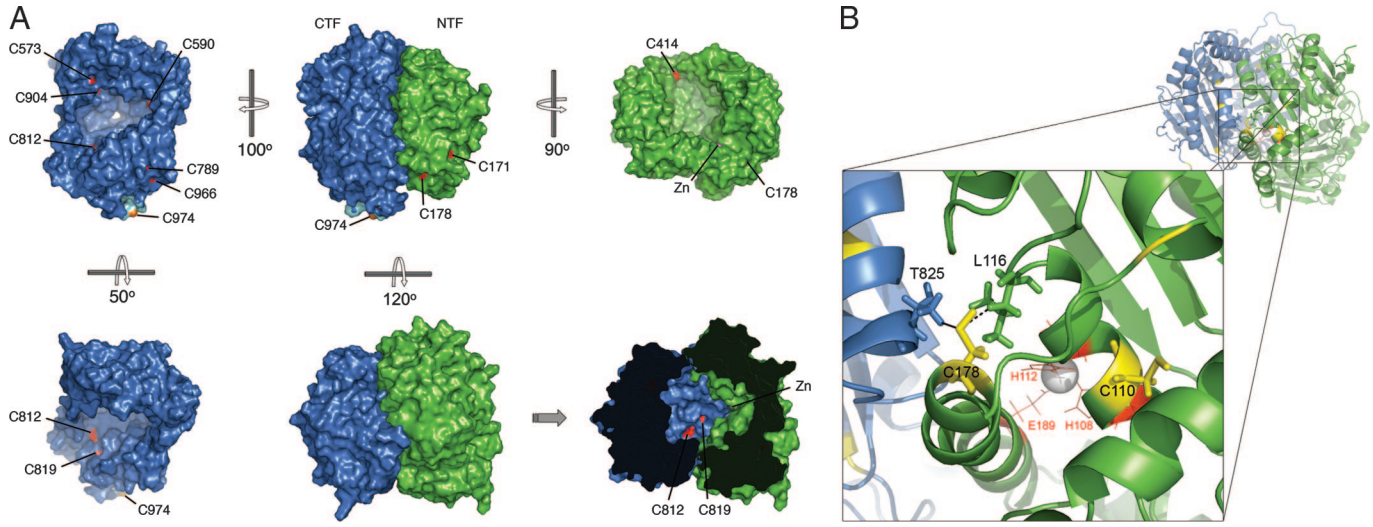

Fig. 1. Cysteine residues present in human IDE. (*A*) Positions of cysteine residues (*red*) accessible to the surface of human IDE as viewed from different perspectives. The N- and C-terminal halves of human IDE are shown in green and blue, respectively, and the zinc atom is depicted as a magenta sphere. The modeled portion of the protein, which includes C974, is depicted in light blue. Note the proximity of C812 and C819 (*red*) to the active-site zinc (*magenta*) when in the closed conformation (*Lower Right*). (*B*) Cysteine residues (*yellow*) near the active site of IDE. Note the placement of C178 near the junction between the N- and C-terminal halves. The zinc atom is depicted as a gray sphere. Dashed lines show the distance between neighboring residues that could be impacted by alkylation. The distances between the sulfur atom in C178 and the nearest atoms in L116 and T825 are 3.02 Å and 5.69 Å, respectively. The figure was constructed from Protein Data Bank ID code 2G54 (20) by using PyMOL (32).

mologs contain a cysteine within their active-site motif (HxCEH) that is absent from the thiol-insensitive bacterial homolog, pitrilysin (also called *Escherichia coli* protease III) (15). Rosner and co-workers (26) mutated this residue (C110) to serine or glycine, but this failed to eliminate the sensitivity of human IDE to NEM. Conversely, Becker and Roth (15) introduced a cysteine into the corresponding site of pitrilysin, but doing so failed to confer thiol sensitivity to the protease. These findings suggested that C110 likely pointed away from the active site, a conclusion that has since been confirmed by crystallographic analysis (20).

In the present work, we used a comprehensive approach to establish which of the 13 cysteine residues within IDE mediate(s) the inactivation of the protease by thiol-alkylating compounds. Our analysis implicates C178, C812, and C819 as the principal residues mediating this effect. These results were unexpected in that they implicate residues quite distal to the residues involved in zinc binding (H108, H112, and E189) and catalysis (E111), providing evidence that the active site of IDE consists of separate halves that must come into close apposition to be fully functional. In addition, we show that alkylation of particular cysteines yields highly substrate-selective effects, including selective activation of the hydrolysis of Aβ with no corresponding effects on insulin, providing insights into the unusual mode of substrate binding of IDE that may aid the development of substrate-selective modulators. Finally, the cysteine-free mutant of IDE generated in this work should have broad utility for numerous applications, including studies investigating whether oxidative damage to IDE could play a role in the pathogenesis of AD and/or DM2.

Results

There are 13 cysteines in known nonmitochondrial isoforms of human IDE (20), including a recently identified splice variant referred to as IDE-15b (27) [Fig. 1*A*, Table 1, and supporting information (SI) Fig. S1]. One additional cysteine, C32, is present within the mitochondrial targeting sequence (Fig. S1*A*). Interestingly, based on the predicted cleavage site within the mitochondrial presequence, C32 is expected to be the extreme N-terminal amino acid within mature mitochondrial IDE isoforms (Fig. S1*A*) (18). Individual cysteines within human IDE show variable degrees of conservation, with several conserved even in invertebrate and unicellular fungal homologs (Table 1 and Fig. S1).

Newly revealed crystal structures of human IDE (20) now permit us to establish the precise location of each cysteine and thereby judge potential mechanisms by which thiol alkylation might lead to inactivation of proteolytic activity. All but two cysteines (C110 and C257) are predicted to be exposed to the surface to some extent (Fig. 1*A* and Table 1). Five cysteines (C573, C590, C812, C819, and C904) face the internal chamber of IDE, whereas five others (C171, C178, C414, C789, and C966) are exposed to the outer surface of the protease (Fig. 1). The location of C974 was not resolved in the crystal structures obtained to date; however, we predict that this residue is also exposed to the outer surface of IDE based on modeling and the assumption of flexibility in this region (Fig. 1*A*). As considered in greater detail below, the position of C178 is of special interest because of its placement at the junction between the N- and C-terminal halves of IDE and its proximity to active-site residues (Fig. 1*B*). Cysteines involved in disulfide bonds represent an additional category of interest. In this regard, it is of interest that C573 and C904 lie quite close in the structures obtained to date (Fig. S2), which we note were determined under reducing conditions (20). If C573 and C904 do form a disulfide bond in the native protein, alkylation could potentially lead to allosteric changes affecting activity. We note that none of the cysteines within IDE makes sufficiently close contact at the homodimer interface to participate in intermolecular disulfide bonds (20). From this structural analysis, we can conclude that thiol-alkylating compounds could influence IDE activity via a large number of potential mechanisms. Moreover, virtually any of the 13 cysteines within IDE, and quite possibly multiple residues, could conceivably be involved, therefore necessitating a comprehensive analysis.

As an initial approach, we generated recombinant IDE in which single cysteines were mutated individually to serine, a structurally similar but much less nucleophilic amino acid (Fig.

Table 1. Cysteine residues present in human IDE and their associated properties

Region	Residue	Species conserved in*	Location†	Comments
N-term	C32	*Mm*	MTS	At N-term in mature mitochondrial isoforms
	C110	*Mm, Xl, Dr, Dm, Ce, Sc*	B	In active-site primary sequence (HFCEH)
	C171	*Mm, Xl, Dr, Sc*	E	
	C178	*Mm, Xl, Dr*	E/B/J	Near zinc-binding residue (E189)
	C257	*Mm, Xl, Dr, Ce, Sc*	B	
	C414	*Mm, Xl, Dr, Dm*	E	
C-term	C573	*Mm, Xl, Dr, Dm*	I	Could form disulfide bridge with C904
	C590	*Mm, Xl, Dr, Dm*	I	Conserved in alternative exon 15b
	C789	*Mm, Xl, Dr* (*Dm, Ce, Sc*)‡	E/B	
	C812	*Mm, Xl, Dr*	I	
	C819	*Mm, Xl, Dr, Dm, Sc*	I	
	C904	*Mm, Xl, Dr*	I	Could form disulfide bridge with C573
	C966	*Mm, Dr*	E	
	C974		E (pred)	Position not resolved by crystallography

**Mm*, *Mus musculus*; *Xl*, *Xenopus laevis*; *Dr*, *Danio rerio*; *Dm*, *Drosophila melanogaster*; *Sc*, *Saccharomyces cerevisae*; *Ce*, *Ceanorhabditis elegans*.
†B, buried; E, external surface; I, internal surface; J, junction between N- and C-terminal halves; MTS, mitochondrial targeting sequence; pred, predicted.
‡Cysteines are present at adjacent position in these species.

2*B*). The 13 different C-to-S mutants, together with wild-type IDE (WT-IDE), were each expressed recombinantly and tested for sensitivity to a range of concentrations of NEM by using an activity assay based on a fluorogenic peptide substrate, FRET1 (see *Materials and Methods*). Like WT-IDE, each of the mutants was fully inhibited by the highest concentration of NEM tested (2 mM; data not shown). This result demonstrates that no single cysteine is wholly responsible for the inactivating effect of NEM, including C110 within the active-site motif, as was shown in ref. 26. However, mutation of C178 to serine or alanine shifted the IC_{50} of NEM by ≈200%, whereas a similar albeit less pronounced effect was observed for IDE-C819S (Fig. 2), thus implicating both of these residues as partially mediating the thiol sensitivity of IDE.

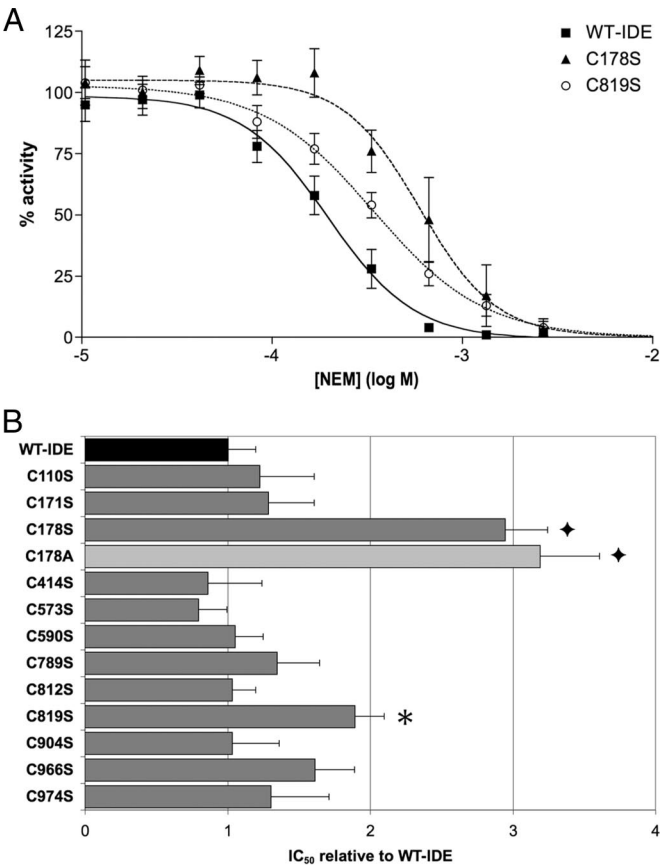

Fig. 2. Effect of individual C-to-S mutations on NEM-mediated inhibition of IDE. (*A*) Dose–response curves showing the activity of IDE-C178S, IDE-C819S, and WT-IDE in the presence of varying concentrations of NEM. (*B*) Graph depicting the IC_{50} values of individual C-to-S mutants relative to WT-IDE. Data are mean ± SEM for 3–14 replications per condition. *, $P < 0.05$; ♦, $P < 0.001$.

Our next strategy was to perform the inverse experiment: namely, generating a cysteine-free IDE mutant (CF-IDE) in which all 13 cysteines were converted to serines, then replacing each cysteine individually. (For clarity, the single-C IDE mutants are designated as IDE-sC110, IDE-sC171, etc.) In principle, this approach should determine which residue(s) are sufficient to impart thiol sensitivity, allowing us to determine more quickly which combination of cysteines underlies this property. Generating CF-IDE would also rule out the more remote possibility that residues other than cysteines might mediate sensitivity to NEM, as has been shown, for example, for vitamin K-dependent carboxylase (28). As expected, near-total resistance to NEM was observed for CF-IDE (Fig. 3). We note, however, that 2 mM NEM consistently produced partial inhibition (≈25%) of CF-IDE and other mutants showing resistance to NEM, suggesting that noncovalent modes of inhibition are operative at this very high concentration.

When the single-C IDE mutants were tested after treatment with 2 mM NEM, we observed significant inhibition for IDE-sC812 and IDE-sC819 (Fig. 3*B*), demonstrating convincingly that C812 and C819 are each sufficient to mediate the inhibition conferred by NEM. However, contrary to inferences derived from previous experiments, IDE-sC178 remained resistant to NEM. To investigate this discrepancy and to determine the minimal set of mutated cysteines necessary to confer resistance to NEM, we examined a large set IDE mutants containing various numbers of C-to-S substitutions distributed throughout the protein (Fig. 4). Consistent with the involvement of C178 seen before (Fig. 2), mutation of C812 and C819 separately or together was not sufficient to produce resistance to NEM; instead, complete resistance to NEM was achieved if and only if C178 was mutated together with both C812 and C819 (Fig. 4). Possible explanations for the inconsistent results obtained with IDE-sC178 are considered below (see *Discussion*).

To establish whether these results were generalizable to more physiologically relevant substrates, the single-C IDE mutants were tested by using Aβ and insulin degradation assays. The

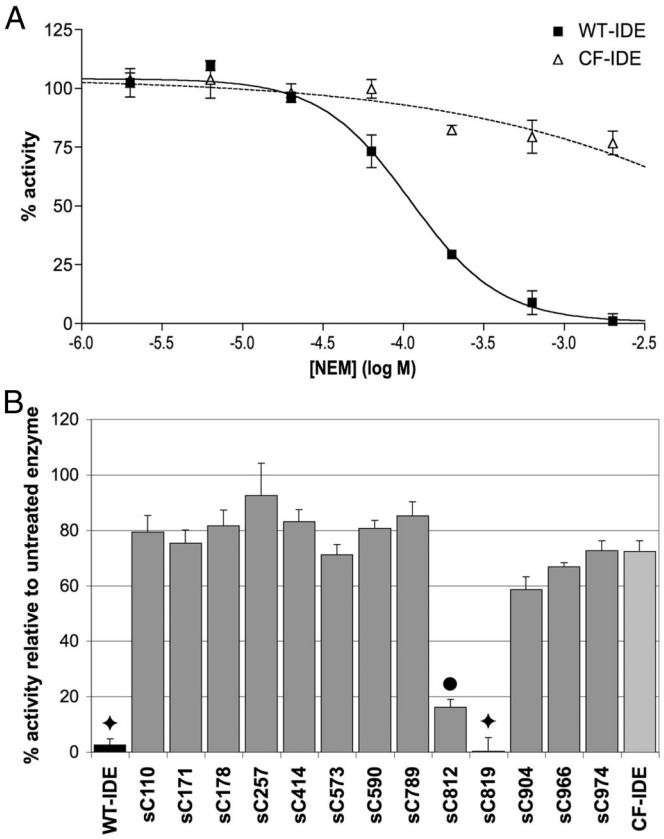

Fig. 3. Effects of NEM on the activity of CF-IDE and single-C IDE mutants. (*A*) Dose–response curves showing the activity of WT-IDE and CF-IDE in the presence of varying concentrations of NEM. Note that, despite strong resistance to NEM, CF-IDE is partially inhibited at high concentrations. (*B*) Graph depicting the activity of single-C mutants in the presence of 2 mM NEM relative to WT-IDE and CF-IDE. Data are mean ± SEM for three to five replications per condition. ●, $P < 0.01$; ♦, $P < 0.001$.

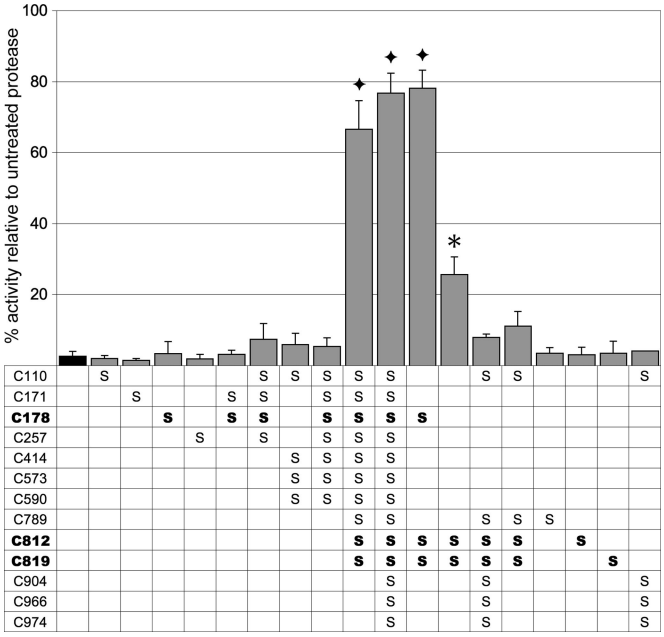

Fig. 4. Effects of NEM on the activity of IDE mutants containing various C-to-S mutations. Graph shows activity for IDE containing C-to-S mutations at the sites indicated in the table below. Note that resistance to NEM is observed if and only if mutations are present in C178, C812, and C819 simultaneously. Data are mean ± SEM for three to six replications per condition. *, $P < 0.05$; ♦, $P < 0.001$.

single-C mutants were especially valuable for probing the molecular details of substrate binding because they permitted the introduction of modifications at several discrete locations distributed throughout the internal chamber of IDE (Fig. 1*A*). Using Aβ or insulin as substrate, IDE-sC812 and IDE-sC819 also showed sensitivity to 2 mM NEM; however, the magnitude of this effect was greatly attenuated for both substrates relative to that observed by using FRET1 (Fig. 5). As was true for FRET1 (Fig. 4), NEM failed to inhibit the hydrolysis of Aβ or insulin by IDE-sC178 (Fig. S3). Finally, in an unexpected result, we found that treatment of IDE-sC590 with NEM significantly activated the hydrolysis of Aβ by ≈44% (Fig. 5) while showing no effect on insulin or FRET1 (Fig. 5). The implications of this surprising finding are considered below.

Discussion

In the present work, we used site-directed mutagenesis and protease activity assays with multiple substrates to probe the role of cysteine residues in determining the well known sensitivity of IDE to thiol-alkylating agents. With some important caveats considered below, our results support the conclusion that C178, C812, and C819 are the principal residues mediating the thiol sensitivity of IDE. Although the evidence implicating C812 and C819 is highly consistent, our results for C178 were less straightforward. On the one hand, mutation of C178 alone imparted a significant rightward shift to the dose–response curve for NEM inhibition. Moreover, mutation of C812 and C819 together was insufficient to confer complete resistance to NEM unless C178 was also mutated. However, contrary to expectations, IDE-sC178 remained resistant to NEM, suggesting that this amino acid was not a sufficient mediator of thiol sensitivity.

What accounts for this discrepancy? We speculate that the position of the lone cysteine in IDE-sC178 is subtly altered by the presence of the 12 C-to-S mutations at the remaining positions in this mutant. Differences in the physicochemical properties between serine and cysteine, particularly when distributed at 12

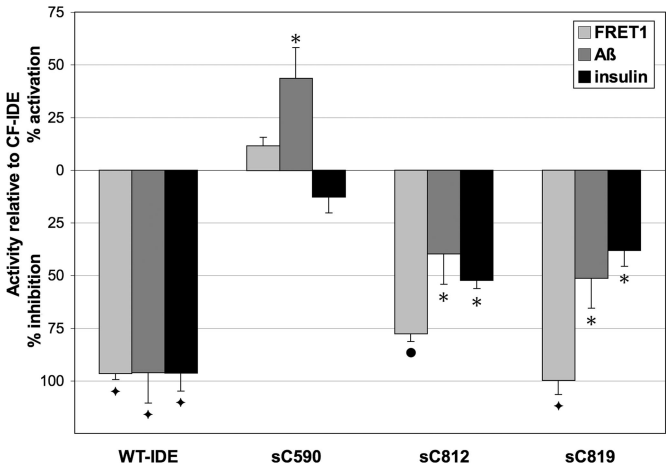

Fig. 5. Substrate-specific effects induced by alkylation of individual cysteines in IDE. Graph depicts the percentage of activation or inhibition observed by using different single-C mutants and different substrates after treatment with 2 mM NEM. Data are presented as the percentage of the activity of CF-IDE under the same condition (see Fig. S3 for the raw dataset). Data are mean ± SEM for three to five replications per condition. Statistical significance reflects comparison with the activity of CF-IDE using the same substrate. *, $P < 0.05$; ●, $P < 0.01$; ♦, $P < 0.001$.

different sites throughout the protein, could influence the positioning of the sulfur atom within C178 and thereby alter its susceptibility to alkylation. C178 is only partially exposed to the surface in WT-IDE (Fig. 1*B*), so even modest changes in position might decrease its vulnerability to alkylation. Consistent with this explanation, we were unable to detect alkylation at C178 by mass spectrometry even after extensive treatment of natively folded IDE-sC178 with NEM (data not shown).

Having determined the specific cysteines mediating the thiol sensitivity of IDE, it nonetheless remains to be established which molecular mechanism(s) are operative, because distinct mechanisms are plausible depending on the precise location of each residue. C812 and C819 are both located on the surface of the internal chamber of IDE (see Fig. 1*A*). In terms of primary structure, these residues are ≈700 aa away from the residues involved in zinc binding and catalysis (H108–H112); nevertheless, they actually lie remarkably close to the active-site zinc at the tertiary structural level (Fig. 1*A Lower Right*). Several conclusions derive from the peculiar placement of these residues. First, because alkylation of either of these residues virtually eliminated hydrolysis of FRET1, it follows that this substrate interacts with this region of the protease. In this instance, the underlying inhibitory mechanism involves interference with the binding of the substrate. It is remarkable, however, that alkylation at these positions failed to abrogate hydrolysis of larger peptide substrates (see Fig. 3*B*). Thus, unlike conventional proteases, there is no single substrate-binding site within IDE that is shared by all substrates; instead, individual substrates appear to interact with any of several domains within the protease in an idiosyncratic manner. This important property of IDE raises the possibility that substrate-selective pharmacological agents might eventually be found.

Our findings with C812 and C819 also provide compelling functional evidence that the active site of IDE is comprised of two separate pieces that become functional only when in close apposition, as obtains exclusively for the closed conformation. It follows that substrate binding can occur only after transition to the closed conformation, and therefore binding likely requires substantial repositioning of the substrate while it is entrapped within the internal chamber. Taken together, these inferences support the interesting proposition that IDE may be capable of cleaving its substrates at multiple sites during a single catalytic cycle.

The contribution of C178 to the thiol sensitivity of IDE likely involves a different set of mechanisms because this residue faces the outer surface of the protease and is also positioned near the interface between the N-and C-terminal halves (see Fig. 1*B*). Because of this peculiar placement, alkylation of C178 could inhibit IDE through two possible mechanisms involving interactions with neighboring residues. The first mechanism involves allosteric changes to the position of active-site residues. C178 resides on the same α-helix containing the zinc-binding residue, E189 (Fig. 1*B*). In addition, the sulfur atom of C178 is positioned very close to L116, which itself lies on the same α-helix containing the remaining three active-site residues (Fig. 1*B*). As was demonstrated recently for IDE, even small changes to active-site moieties can have profound influences on the behavior of the protease (29). A second possible mechanism follows from the proximity of C178 to T825 (Fig. 1*B*). Because T825 lies within the C-terminal half of IDE, it is likely that alkylation of C178 disrupts the close apposition of the C- and N-terminal regions required for full functionality. Whether either or both of these mechanisms apply, both can be conceived of as allosteric effects that indirectly alter the shape of the active site.

An unexpected finding of the present work was the discovery that alkylation of C590 significantly accelerated the hydrolysis of Aβ but not insulin or our fluorogenic peptide substrate. This result constitutes an intriguing example of activation of IDE by a synthetic small molecule and, more generally, provides an important proof of principle showing that IDE activity can indeed be modulated bidirectionally and substrate-selectively. From a therapeutic perspective, this result is also of interest in that it specifically implicates the region surrounding C590 as differentially involved in the binding of Aβ but not insulin. It is conceivable that selective modification of this region, either pharmacologically or by mutation, could lead to the selective enhancement of Aβ degradation. However, it remains to be determined whether this can be achieved in practice.

In view of the substrate-selective effects we have observed, it is important to qualify our conclusions as strictly applying only to those substrates specifically investigated in this work. We cannot exclude the possibility that alkylation of cysteines other than C178, C812, and C819 may inhibit the processing of substrates we did not test or, conversely, that alkylation at these sites might fail to inhibit the processing of other substrates. In a related vein, it is also important to recognize that the properties of the thiol-alkylating agent itself will strongly influence whether or not inhibition or activation is achieved with a particular substrate.

By way of conclusion, we would like to highlight the practical utility of the cysteine-free mutant we have developed, CF-IDE. By introducing cysteine(s) at appropriate positions, CF-IDE can be modified site-specifically with a wide range of thiol-selective reagents. Such an approach would be used for exploring substrate–protease interactions or for many other possible applications. In addition, CF-IDE should prove invaluable in future studies investigating whether oxidative damage to IDE cysteines might play a role in the etiology of AD or DM2.

Materials and Methods

Site-Directed Mutagenesis. Mutations were introduced into pGST-wtIDE, a bacterial expression vector encoding wild-type IDE fused to the C terminus of GST (27), by using the QuikChange site-directed mutagenesis kit according to the manufacturer's recommendations (Stratagene). Mutations were verified by DNA sequencing. To minimize the possible accrual of secondary mutations in the vector backbone, mutated portions of cDNAs were cloned back into the original vector by using appropriate restriction sites. A similar domain-swapping cloning strategy was used to generate CF-IDE and other multiple C-to-S mutants.

IDE Expression and Purification. Expression and purification of IDE were carried out as described in ref. 27. Mutants were stored frozen at −80°C in storage buffer [50 mM Tris (pH 7.4), 100 mM NaCl, 1 mM DTT]. Immediately before activity assays, the storage buffer was exchanged with DTT-free assay buffer [50 mM HEPES (pH 7.0), 100 mM NaCl, 10 mM $MgCl_2$ supplemented with 0.1% BSA] by using 0.5-ml Amicon Microcon YM-30 spin columns according to the manufacturer's recommendations (Millipore Corp.). To control for the time-dependence of NEM-mediated inhibition, all proteases were preincubated with NEM for an identical time period (1 h) before the initiation of reactions.

Activity Assays. IDE activity was quantified as described in ref. 30 by monitoring the rate of hydrolysis of (7-methoxycoumarin-4-yl)acetic acid-GGFLRKVGQK(2,4-dinitrophenyl) (FRET1; 5 μM), a fluorogenic peptide substrate (kindly synthesized by Margaret Condron and David Teplow, UCLA). Aβ degradation was measured by using a fluorescence polarization-based assay as described in ref. 31. Insulin degradation was assessed by quantifying hydrolysis-dependent fluorescence dequenching (λ_{ex}, 485; λ_{em}, 535) of insulin labeled with fluorescein isothiocyanate (50 nM; Sigma). Assays were performed at room temperature in black, 384-well, low-volume nonbinding surface microplates (Corning, Inc.) by using a SpectraMax M5 multimode spectrophotometer (Molecular Devices).

Statistical Analysis. Tests for statistical significance were performed by using the two-tailed Student's *t* test with various levels of significance ($P = 0.05$, 0.01, or 0.001). For comparisons with unequal numbers of replications per group, Hartley's F_{max} was calculated to check for homogeneity of variance.

ACKNOWLEDGMENTS. We thank Drs. Margaret Condron and David Teplow for synthesizing FRET1, Ms. Anna Leech and Mrs. Qun Lu for assistance with cloning and protein expression, and Dr. Wei-Jen Tang for helpful discussions. This work was supported by National Institutes of Health Grants AG025070 (to M.A.L.) and AG12749 (to M.A.L. and D.J.S.), by the Ellison Medical Foundation (to M.A.L.), and by a generous donation from The Unforgettable Fund (to M.A.L. and M.N.-F.).

1. Tanzi RE, Moir RD, Wagner SL (2004) Clearance of Alzheimer's Aβ peptide: The many roads to perdition. *Neuron* 43:605–608.
2. Hersh LB (2006) The insulysin (insulin-degrading enzyme) enigma. *Cell Mol Life Sci* 63:2432–2434.
3. Leissring MA, Saido TC (2007) in *Alzheimer's Disease*: *Advances in Genetics, Molecular and Cellular Biology*, eds Sisodia S, Tanzi R (Springer, New York), pp 157–178.
4. Bertram L, *et al.* (2000) Evidence for genetic linkage of Alzheimer's disease to chromosome 10q. *Science* 290:2302–2303.
5. Myers A, *et al.* (2000) Susceptibility locus for Alzheimer's disease on chromosome 10. *Science* 290:2304–2305.
6. Ertekin-Taner N, *et al.* (2000) Linkage of plasma Aβ42 to a quantitative locus on chromosome 10 in late-onset Alzheimer's disease pedigrees. *Science* 290:2303–2304.
7. Ott A, *et al.* (1999) Diabetes mellitus and the risk of dementia: The Rotterdam Study. *Neurology* 53:1937–1942.
8. Zeggini E, *et al.* (2007) Replication of genome-wide association signals in UK samples reveals risk loci for type 2 diabetes. *Science* 316:1336–1341.
9. Sladek R, *et al.* (2007) A genome-wide association study identifies novel risk loci for type 2 diabetes. *Nature* 445:881–885.
10. Farris W, *et al.* (2004) Partial loss-of-function mutations in insulin-degrading enzyme that induce diabetes also impair degradation of amyloid β-protein. *Am J Pathol* 164:1425–1434.
11. Fakhrai-Rad H, *et al.* (2000) Insulin-degrading enzyme identified as a candidate diabetes susceptibility gene in GK rats. *Hum Mol Genet* 9:2149–2158.
12. Farris W, *et al.* (2003) Insulin-degrading enzyme regulates the levels of insulin, amyloid β-protein, and the β-amyloid precursor protein intracellular domain *in vivo*. *Proc Natl Acad Sci USA* 100:4162–4167.
13. Miller BC, *et al.* (2003) Amyloid-β peptide levels in brain are inversely correlated with insulysin activity levels *in vivo*. *Proc Natl Acad Sci USA* 100:6221–6226.
14. Leissring MA, *et al.* (2003) Enhanced proteolysis of β-amyloid in APP transgenic mice prevents plaque formation, secondary pathology, and premature death. *Neuron* 40:1087–1093.
15. Becker AB, Roth RA (1995) Insulysin and pitrilysin: Insulin-degrading enzymes of mammals and bacteria. *Methods Enzymol* 248:693–703.
16. Roth RA (2004) in *Handbook of Proteolytic Enzymes*, eds Barrett AJ, Rawlings ND, Woessner JF (Elsevier, London), pp 871–876.
17. Becker AB, Roth RA (1992) An unusual active site identified in a family of zinc metalloendopeptidases. *Proc Natl Acad Sci USA* 89:3835–3839.
18. Leissring MA, *et al.* (2004) Alternative translation initiation generates a novel isoform of insulin-degrading enzyme targeted to mitochondria. *Biochem J* 383:439–446.
19. Vekrellis K, *et al.* (2000) Neurons regulate extracellular levels of amyloid β-protein via proteolysis by insulin-degrading enzyme. *J Neurosci* 20:1657–1665.
20. Shen Y, Joachimiak A, Rosner MR, Tang W-J (2006) Structures of human insulin-degrading enzyme reveal a new substrate recognition mechanism. *Nature* 443:870–874.
21. Garcia JV, Fenton BW, Rosner MR (1988) Isolation and characterization of an insulin-degrading enzyme from *Drosophila melanogaster*. *Biochemistry* 27:4237–4244.
22. Kim M, *et al.* (2007) Decreased catalytic activity of the insulin-degrading enzyme in chromosome 10-linked Alzheimer's disease families. *J Biol Chem* 282:7825–7832.
23. Zhao Z, *et al.* (2007) Insulin-degrading enzyme activity selectively decreases in the hippocampal formation of cases at high risk to develop Alzheimer's disease. *Neurobiol Aging* 28:824–830.
24. Caccamo A, *et al.* (2005) Age- and region-dependent alterations in Aβ-degrading enzymes: Implications for Aβ-induced disorders. *Neurobiol Aging* 26:645–654.
25. Ding L, Becker AB, Suzuki A, Roth RA (1992) Comparison of the enzymatic and biochemical properties of human insulin-degrading enzyme and *Escherichia coli* protease III. *J Biol Chem* 267:2414–2420.
26. Perlman RK, Gehm BD, Kuo WL, Rosner MR (1993) Functional analysis of conserved residues in the active site of insulin-degrading enzyme. *J Biol Chem* 268:21538–21544.
27. Farris W, *et al.* (2005) Alternative splicing of human insulin-degrading enzyme yields a novel isoform with a decreased ability to degrade insulin and amyloid β-protein. *Biochemistry* 44:6513–6525.
28. Rishavy MA, *et al.* (2004) A new model for vitamin K-dependent carboxylation: The catalytic base that deprotonates vitamin K hydroquinone is not Cys but an activated amine. *Proc Natl Acad Sci USA* 101:13732–13737.
29. Song ES, *et al.* (2005) Mutation of active site residues of insulin-degrading enzyme alters allosteric interactions. *J Biol Chem* 280:17701–17706.
30. Im H, *et al.* (2007) Structure of substrate-free human insulin-degrading enzyme (IDE) and biophysical analysis of ATP-induced conformational switch of IDE. *J Biol Chem* 282:25453–25463.
31. Leissring MA, *et al.* (2003) Kinetics of amyloid β-protein degradation determined by novel fluorescence- and fluorescence polarization-based assays. *J Biol Chem* 278:37314–37320.
32. DeLano WL (2002) The PyMOL Molecular Graphics System (DeLano Scientific, Palo Alto, CA).
33. Shinall H, Song ES, Hersh LB (2005) Susceptibility of amyloid beta peptide degrading enzymes to oxidative damage: A potential Alzheimer's disease spiral. *Biochem* 44:15345–15350.